Naval Research Laboratory
Washington, DC 20375-5320

NRL/5310/MR—2024/3

Wrapped-Lattice Cylindrical Arrays and Their Phase Modes, Basic Theory

JEFFREY O. COLEMAN (RETIRED)

WILLIAM MARK DORSEY

Antenna Section
Radar Division

March 25, 2024

REPORT DOCUMENTATION PAGE

PLEASE DO NOT RETURN YOUR FORM TO THE ABOVE ORGANIZATION

1. REPORT DATE	2. REPORT TYPE	3. DATES COVERED	
		START DATE	END DATE
25-03-2024	NRL Memorandum Report	01/01/2017	02/21/2024

4. TITLE AND SUBTITLE
Wrapped-Lattice Cylindrical Arrays and Their Phase Modes, Basic Theory

5a. CONTRACT NUMBER	5b. GRANT NUMBER	5c. PROGRAM ELEMENT NUMBER
5d. PROJECT NUMBER	**5e. TASK NUMBER**	**5f. WORK UNIT NUMBER**
		6B10

6. AUTHOR(S)
Jeffrey O. Coleman* and William Mark Dorsey

7. PERFORMING ORGANIZATION / AFFILIATION NAME(S) AND ADDRESS(ES)
Naval Research Laboratory
4555 Overlook Ave SW
Washington, DC 20375-5320

8. PERFORMING ORGANIZATION REPORT NUMBER
NRL/5310/MR—2024/3

9. SPONSORING / MONITORING AGENCY NAME(S) AND ADDRESS(ES)	10. SPONSOR / MONITOR'S ACRONYM(S) NUMBER	11. SPONSOR / MONITOR'S REPORT NUMBER(S)
Naval Research Laboratory 4555 Overlook Ave SW Washington, DC 20375-5320	NRL	

12. DISTRIBUTION / AVAILABILITY STATEMENT
DISTRIBUTION STATEMENT A: Approved for public release; distribution is unlimited.

13. SUPPLEMENTAL NOTES
*Retired

14. ABSTRACT
Taylor's 1952 approach to steering a uniform circular array (UCA) used a discrete-Fourier-transform (DFT) of the element outputs to create signals now routinely termed phase modes. This work derives an analogous phase-mode representation and steering approach for a cylindrical array in which elements are nominally located on a 2D lattice, which need not be separable, wrapped around the cylinder. The DFT becomes a generalized DFT on a lattice with the DFT sum indexed on a family of coset representatives. This is preliminary work and does not yet include computational simulation or experimental results.

15. SUBJECT TERMS
Cylindrical arrays, Conformal arrays, Phase modes

16. SECURITY CLASSIFICATION OF:			17. LIMITATION OF ABSTRACT	18. NUMBER OF PAGES
a. REPORT	b. ABSTRACT	c. THIS PAGE		
U	U	U	SAR	24

19a. NAME OF RESPONSIBLE PERSON	19b. PHONE NUMBER *(Include area code)*
William Mark Dorsey	(202) 404-5639

This page intentionally left blank.

CONTENTS

This page intentionally left blank.

WRAPPED-LATTICE CYLINDRICAL ARRAYS AND THEIR PHASE MODES, BASIC THEORY

1. INTRODUCTION

In a receive context the *phase modes* of a uniform circular array (UCA) are the outputs of a discrete Fourier transform (DFT) driven by the UCA's element outputs. It's well established that these phase modes can be weighted and summed to create array patterns steerable with linear phases much like uniform line arrays [1, 2, 3]. Even when not used directly for implementation, the phase-mode formulation turns out to offer insights into array parameter selection [4]. As an intended first step towards obtaining similar benefits for cylindrical arrays, this report develops a structurally similar phase-mode formulation for cylindrical arrays in which nominal element locations lie on a point lattice wrapped around a cylinder.

Let us first walk briefly through the UCA phase-mode derivation to orient ourselves to the task ahead. Key equations will be flagged parenthetically with the numbers of corresponding equations in the general cylindrical-array formulation to follow.

1.1 UCA Theory

The few very short initial sections here simply synchronize this UCA development with the cylindrical-array development to follow in Section 2.1.

1.1.1 Antennas and their Translation in Space (UCA)

Moving an antenna scales its pattern by a complex exponential with an exponent that captures the direction and magnitude of the motion. We won't deal with that explicitly in Section 1.1 at all but will assume that element patterns already incorporate factors associated with motions used in constructing those elements.

1.1.2 Positioning an Antenna on the Circle (UCA)

In this development there is no shifting of elements out from the origin to locate them on the circle. All patterns are for structures mathematically at the origin, even when their implementations involve physical structures extending out some distance from it. Readers who think in terms of phase centers can imagine starting with an element with phase center at the origin and then shifting that phase center out to the circle to obtain the element considered here, one with an origin-referenced pattern that includes the likely considerable effects of that shift.

1.1.3 Locate Array Elements on a Circle (UCA)

The UCA is assumed centered at the origin with N elements uniformly spaced in azimuth ϕ and numbered $0, \ldots, N-1$ in the direction of increasing azimuth and beginning at nominal pointing direction $\phi = 0$.

Manuscript approved March 21, 2024.

1.1.4 The Array Pattern's Several Basic Forms (UCA)

A Fourier-Series Prototype Element Pattern (UCA)

First, write a prototype element pattern for the polarization of interest as a Fourier series in azimuth ϕ,

$$P(\phi) = \sum_k a_k \, \mathrm{e}^{jk\phi} \tag{1}$$

(parallels (34) below). In this report sums from $-\infty$ to ∞, i.e. over all of $\mathbb{Z}$, are shown without limits.

For a given incoming wave, we assume polarization reference directions that rotate in azimuth with the direction of wave propagation so that the pattern $P_n(\phi)$ of the nth of the array's N elements is just this prototype pattern shifted in azimuth to the element's actual position on the circle. So

$$P_n(\phi) \triangleq P(\phi - 2\pi n/N) = \sum_k a_k \, \mathrm{e}^{-j2\pi kn/N} \, \mathrm{e}^{jk\phi} \tag{2}$$

(parallels (35) and (36) below).

Ordinary Array-Pattern Sum (UCA)

Combining complex element outputs using complex weights $\{w_n\}$ yields an array output with a corresponding pattern obtained as a similarly weighted sum of the element patterns:

$$C(\phi) \triangleq \sum_{n=0}^{N-1} w_n P_n(\phi) \tag{3}$$

$$= \sum_k a_k \sum_{n=0}^{N-1} w_n \, \mathrm{e}^{-j2\pi kn/N} \, \mathrm{e}^{jk\phi} \tag{4}$$

$$= \sum_k a_k \, W(k/N) \, \mathrm{e}^{jk\phi} \tag{5}$$

(parallels (37), (38), and (39) below), using (2) in (4). Here (5) uses discrete-time Fourier transform (DTFT)

$$W(f) \triangleq \sum_{n=0}^{N-1} w_n \, \mathrm{e}^{-j2\pi fn} \tag{6}$$

(parallels (40) below) of element weights w_n and in so doing encourages the interpretation of UCA pattern (5) as a Fourier series in azimuth with coefficients that are [1] just the element-pattern coefficients times a sampled DTFT of the array's complex combining weights. (Yes, that sampled DTFT is a DFT. We'll formally make that connection shortly.)

Phase-Mode Pattern Sum (UCA)

Yet another Fourier domain yields an alternative to (4) and (5). Take a discrete Fourier transform (DFT) of the element outputs to obtain N *phase-mode* outputs with the mth having the phase-mode pattern, for $0 \leq m < N$, given by

$$Y_m(\phi) \triangleq \sum_{n=0}^{N-1} P_n(\phi)\, \mathrm{e}^{-j2\pi mn/N} \tag{7}$$

(parallels (41) below). We can likewise transform the weights to define

$$W_m \triangleq \sum_{n=0}^{N-1} w_n\, \mathrm{e}^{-j2\pi mn/N} \tag{8}$$

(parallels (42) below). Definitions (7) and (8) of $Y_m(\phi)$ and W_m easily extend periodically to $m \in \mathbb{Z}$ with one period comprising $\{0, \ldots, N-1\}$. We just use decomposition $m = (m \bmod N) + m'N$ to replace m on the right with $m \bmod N$. The exponential's periodicity makes $m'N$ irrelevant for every $m' \in \mathbb{Z}$.

Applying an inverse DFT to (7),

$$P_n(\phi) = \frac{1}{N} \sum_{m=0}^{N-1} Y_m(\phi)\, \mathrm{e}^{\,j2\pi mn/N}$$

which in (3) yields, after a little reordering,

$$C(\phi) = \frac{1}{N} \sum_{m=0}^{N-1} \Big(\sum_{n=0}^{N-1} w_n\, \mathrm{e}^{\,j2\pi mn/N} \Big) Y_m(\phi).$$

Using DFT (8) to rewrite the contents of the parentheses,

$$C(\phi) = \frac{1}{N} \sum_{m=0}^{N-1} W_{-m} Y_m(\phi) \tag{9}$$

(parallels (43) below). Computationally, subscript $-m$ can be reduced modulo N. Change of basis (7) and (8) relates the equivalent weighted array-pattern sums here and in (3), and the next section will further relate these array-pattern sums through the sampling relationship $W_m = W(m/N)$ that connects (6) and (8).

1.1.5 Simple, Approximate Steering (UCA)

A key goal of this entire development is simple, if approximate, azimuth steering. In the UCA case the approach here generally follows [4], a modern presentation of an approach of Sheleg [2].

Ideally, azimuth steering by ϕ_s would replace ϕ with $\phi - \phi_s$ in array pattern $C(\phi)$. Can this be done by modifying weights? Replacement in array sum (3) or (9) physically rotates the array by ϕ_s, which is not

helpful, and in (4) it scales w_n by an exponential dependent, unacceptably, on Fourier-series index k. Is the steered pattern even in the space realizable by the sums of (3) and (9)? No. They have only N degrees of freedom and so can synthesize the steered pattern only in very special cases. We must approximate.

Azimuth Steering (UCA)

We begin by recognizing weight DFT (8) in (4) to write

$$C(\phi) = \sum_k a_k W_k \, \mathrm{e}^{\,jk\phi} \tag{10}$$

$$= \sum_k a_k W_{k \bmod N} \, \mathrm{e}^{\,jk\phi} \tag{11}$$

(parallels (46) and (47)). Alternate form (11) emphasizes the periodicity of W_k. Replacing ϕ with $\phi - \phi_s$ in (10) then yields the ideally steered array pattern

$$C(\phi - \phi_s) = \sum_k a_k \, \mathrm{e}^{-jk\phi_s} \, W_k \, \mathrm{e}^{\,jk\phi} \tag{12}$$

(parallels (48)).

Replacing Fourier coefficients a_k with $a_k \, \mathrm{e}^{-jk\phi_s}$ would rotate the element pattern, and indeed the array, by ϕ_s. Here we will approximate that impractical ideal with modified Fourier series

$$C(\phi - \phi_s) \approx \sum_k a_k \, S_k \, W_k \, \mathrm{e}^{\,jk\phi} \tag{13}$$

(parallels (49)) with new quantity S_k of the same period as W_k. In implementation then, W_k in phase-mode pattern sum (9) or the corresponding real-time beamsum can be replaced with product $S_k W_k$. Alternatively, weights w_n in original pattern sum (3) and the corresponding beamsums can be replaced with steered weights w'_n computed using the inverse of DFT (8):

$$w'_n \triangleq \frac{1}{N} \sum_{m=0}^{N-1} S_m W_m \, \mathrm{e}^{\,j2\pi mn/N} \, .$$

The periodicity of S_k is at the heart of how we set it. In (13), the values $k = 0, \ldots, N-1$ comprise a single period of S_k. If we pick one of these intra-period k values and call it m, by periodicity S_k is identical for all $k \in m + \mathbb{Z}N \triangleq \ldots, m-2N, m-N, m, m+N, m+2N, \ldots$ When we choose the value of S_k for any of these k, we are choosing the value of S_k for all of these k, so we cannot set $S_k = \mathrm{e}^{-jk\phi_s}$ for these various k independently. However, if we resolve to set it to a phase factor of some sort so that $|S_k| = 1$, the kth term in (13) then has magnitude $|a_k \, S_k \, W_k \, \mathrm{e}^{\,jk\phi}| = |a_k W_k|$, so if we note the k for which this magnitude is largest, we can set S_k to the ideal value for that k:

$$k_{\text{max}} = \operatorname*{argmax}_{k \in m + \mathbb{Z}N} |a_k W_k| \tag{14}$$

$$S_k = \mathrm{e}^{-jk_{\text{max}}\phi_s} \qquad \text{for all } k \in m + \mathbb{Z}N \tag{15}$$

For these $k \in m + \mathbb{Z}N$ where S_k is forced to be identical then, S_k takes the ideal value for the term in (13) for which it will have the largest effect on the sum. The other terms we can consider error terms. We repeat this assignment procedure for each m in a period, and we are done. We have simple, though likely nonoptimal, steering.

In [4] we show by example, how the N values of $k_{\max}$ are typically a cluster of k values where $|k|$ is smallest and that the right choice of the number N of elements relative to the UCA radius can make the error terms small.

2. BASIC THEORY

2.1 Wrapped-Lattice Cylindrical-Array Theory

This development aims at circuits-and-systems researchers who are comfortable with mathematics and have solid undergraduate electromagnetics exposure but no antenna backgrounds. Notation was chosen accordingly and so conflicts at times with what is usual in the antenna community.

2.1.1 Antennas and their Translation in Space

This short background section develops a simple analytic framework for receive antennas subject to incident electromagnetic fields comprising propagating plane waves in free space. The signals-and-systems approach taken incorporates spatial translation of antennas from the outset in order to prepare for our later analysis of structurally periodic antenna arrays.

Antenna Translation

Suppose a receive antenna spatially translated by vector $\mathbf{x}$ has output $a(\mathbf{x}, t)$. Maxwell's equations make the map from the real incident electric field $\vec{e}(\mathbf{x}, t)$ to $a(\mathbf{x}, t)$ linear, time invariant, and space invariant, the latter because replacing $\vec{e}(\mathbf{x}, t)$ with $\vec{e}(\mathbf{x} - \mathbf{x}_0, t)$ and $a(\mathbf{x}, t)$ with $a(\mathbf{x} - \mathbf{x}_0, t)$, which shifts the original antenna's position by $\mathbf{x}_0$, leaves the outputs at all translations $\mathbf{x}$ unchanged. The output is therefore characterized by a convolution of the form

$$a(\mathbf{x}, t) = \iint \vec{e}(\mathbf{y}, \tau) \cdot \vec{p}(\mathbf{x} - \mathbf{y}, t - \tau)\, d\mathbf{y}\, d\tau \tag{16}$$

using differential volume $d\mathbf{y}$ in the inner integral. The vector-valued impulse response or Green's function $\vec{p}(\mathbf{x}, t)$ acts via a dot product, as scalar $a(\mathbf{x}, t)$ is linear and time/space invariant in each Cartesian component of $\vec{e}(\mathbf{y}, \tau)$. The Fourier integrals

$$\vec{e}(\mathbf{x}, t) = \iint \vec{E}(\boldsymbol{\kappa}, f)\, \mathrm{e}^{j2\pi(ft + \boldsymbol{\kappa}\mathbf{x})}\, df\, d\boldsymbol{\kappa} \tag{17}$$

$$\vec{p}(\mathbf{x}, t) = \iint \vec{P}(\boldsymbol{\kappa}, f)\, \mathrm{e}^{j2\pi(ft + \boldsymbol{\kappa}\mathbf{x})}\, df\, d\boldsymbol{\kappa}$$

$$a(\mathbf{x}, t) = \iint A(\boldsymbol{\kappa}, f)\, \mathrm{e}^{j2\pi(ft + \boldsymbol{\kappa}\mathbf{x})}\, df\, d\boldsymbol{\kappa} \tag{18}$$

take real vector $\boldsymbol{\kappa}$ as 3D spatial frequency, take $\boldsymbol{\kappa}$ and $\mathbf{x}$ to be row and column three-vectors respectively so that $\boldsymbol{\kappa}\mathbf{x}$ is a dot product, and take 3D differential $d\boldsymbol{\kappa}$ to be an inverse volume. The convolution property of the transform and (16) then yield

$$A(\boldsymbol{\kappa}, f) = \vec{E}(\boldsymbol{\kappa}, f) \cdot \vec{P}(\boldsymbol{\kappa}, f). \tag{19}$$

This dot product is not a complex inner product but only a sum of products of corresponding Cartesian components, with no complex conjugation. Here $\vec{P}(\boldsymbol{\kappa}, f)$ denotes a spatio-temporal frequency response or, in other words, an antenna pattern.

Interpretation and Assumptions

Let the incident field comprise plane waves in free space and so have no $f = 0$ component. When $f > 0$ the complex-exponential wave in (17) has wavenumber vector $-2\pi\boldsymbol{\kappa}$, so we term spatial frequency $\boldsymbol{\kappa}$ the *look vector* and say it points in the "look direction" from which the wave is arriving. Vector field $\vec{E}(\boldsymbol{\kappa}, f)$ has as Cartesian components the complex amplitudes of the electric-field wave's Cartesian components. Rewriting (18) and (19) as

$$\begin{aligned} a(\mathbf{x}, t) &= \int \mathrm{A}(\mathbf{x}, f)\, \mathrm{e}^{j2\pi f t}\, df \\ \mathrm{A}(\mathbf{x}, f) &= \int \vec{E}(\boldsymbol{\kappa}, f) \cdot \vec{P}(\boldsymbol{\kappa}, f)\, \mathrm{e}^{j2\pi\boldsymbol{\kappa}\mathbf{x}}\, d\boldsymbol{\kappa} \end{aligned} \tag{20}$$

shows $\vec{P}(\boldsymbol{\kappa}, f)$ and $\vec{P}(\boldsymbol{\kappa}, f)\, \mathrm{e}^{j2\pi\boldsymbol{\kappa}\mathbf{x}}$ to be, according as $\mathbf{x}$ is or is not zero, the complex vector patterns of the original and spatially translated antenna respectively, as their components scale the components of the complex field amplitude when the effects of indicent waves from all directions are combined in the integral in (20). The dot product there captures the sensitivity of the complex pattern to incident-wave polarization.

Assume analytic filtering [5] eliminates any $f < 0$ antenna-output components using filtering referred for this analysis into complex pattern $\vec{P}(\boldsymbol{\kappa}, f)$. Without that assumption, both $\vec{p}(\mathbf{x}, t)$ and (therefore) $a(\mathbf{x}, t)$ in (16) are real, but analytic filtering makes them complex and analytic (no $f < 0$ components). No information is lost, as Fourier relationship $2\,\mathrm{Re}(g(t)) = g(t) + g^*(t) \leftrightarrow G(f) + G^*(-f)$ implies that taking twice its real part will restore the missing spectral components of any analytic signal $g(t)$, though restoration is seldom needed in practice. The analytic filtering simplifies our array sum below.

Let us assume $f > 0$ then, and for notational brevity, let us also drop the f dependence and take the complex field and complex pattern respectively to be row and column Cartesian three-vectors so that $\vec{E}(\boldsymbol{\kappa}) \cdot \vec{P}(\boldsymbol{\kappa})$ becomes just $\vec{E}(\boldsymbol{\kappa})\vec{P}(\boldsymbol{\kappa})$.

By Maxwell's equations, plane-wave $\vec{E}(\boldsymbol{\kappa})$ has no component in the look direction. Further, it is concentrated on (impulsive on) spatial frequencies $\boldsymbol{\kappa}$ satisfying Helmholtz relation $\|\boldsymbol{\kappa}\| = 1/\lambda$, where wavelength $\lambda = c/f$ is determined from the implicit frequency variable as usual. Without loss of generality in (20) then, we assume $\vec{P}(\boldsymbol{\kappa})$ also has no component in the $\boldsymbol{\kappa}$ direction and is defined only where $\|\boldsymbol{\kappa}\| = 1/\lambda$.

Horizontal and Vertical Polarization

Here we avoid the usual "Ludwig" polarization frameworks [6] because their polarization vectors are specified relative to physical antenna orientation and our cylindrical array's elements will be pointed in

many directions. We instead tie polarization directions to the look direction in spherical coordinates. Let the length, azimuth, and elevation of row vector $\boldsymbol{\kappa}$ be r, ϕ, and θ, and let the usual orthogonal dimensionless unit vectors in the directions of their differential increments be row vectors $\widehat{r}$, $\widehat{\phi}$, and $\widehat{\theta}$, the $\boldsymbol{\kappa}$ dependence of which is suppressed notationally for brevity.

As their $\widehat{r}$ components are zero, $\vec{E}(\boldsymbol{\kappa})$ and $\vec{P}(\boldsymbol{\kappa})$ can each be written using two scalar patterns obtained as inner products:

$$\begin{aligned}\vec{E}(\boldsymbol{\kappa}) &= E_{\widehat{\phi}}(\boldsymbol{\kappa})\,\widehat{\phi} \;\; + E_{\widehat{\theta}}(\boldsymbol{\kappa})\,\widehat{\theta} \\ \vec{P}(\boldsymbol{\kappa}) &= P_{\widehat{\phi}}(\boldsymbol{\kappa})\;\widehat{\phi}^{\,T} + P_{\widehat{\theta}}(\boldsymbol{\kappa})\;\widehat{\theta}^{\,T}\end{aligned} \tag{21}$$

$$\begin{aligned} E_{\widehat{\phi}}(\boldsymbol{\kappa}) &\triangleq \vec{E}(\boldsymbol{\kappa})\,\widehat{\phi}^{\,T}, & E_{\widehat{\theta}}(\boldsymbol{\kappa}) &\triangleq \vec{E}(\boldsymbol{\kappa})\,\widehat{\theta}^{\,T} \\ P_{\widehat{\phi}}(\boldsymbol{\kappa}) &\triangleq \widehat{\phi}\,\vec{P}(\boldsymbol{\kappa})\,, & P_{\widehat{\theta}}(\boldsymbol{\kappa}) &\triangleq \widehat{\theta}\,\vec{P}(\boldsymbol{\kappa})\,. \end{aligned} \tag{22}$$

We refer to the scalar patterns $P_{\widehat{\phi}}(\boldsymbol{\kappa})$ and $P_{\widehat{\theta}}(\boldsymbol{\kappa})$ as patterns for horizontal and vertical polarization respectively.

From (20), the unshifted (and unrotated) antenna has output

$$\begin{aligned}\mathrm{A}(0) &= \int \vec{E}(\boldsymbol{\kappa})\vec{P}(\boldsymbol{\kappa})\,d\boldsymbol{\kappa} \\ &= \int E_{\widehat{\phi}}(\boldsymbol{\kappa})P_{\widehat{\phi}}(\boldsymbol{\kappa})\,d\boldsymbol{\kappa} + \int E_{\widehat{\theta}}(\boldsymbol{\kappa})P_{\widehat{\theta}}(\boldsymbol{\kappa})\,d\boldsymbol{\kappa}.\end{aligned} \tag{23}$$

The Form of the Array Pattern

An antenna array is a set of antennas, termed array elements or simply elements, each with a vector pattern or scalar patterns. Using the element outputs of a large array to optimally estimate the parameters of all incident waves simultaneously is rarely computationally feasible, so estimation is conventionally driven with a smaller number of array "beams," each a linear combination of element outputs, linear to avoid intermodulation. A narrowband array, examined here, uses complex combining weights. A wideband array, in contrast, uses complex frequency responses—filters—instead. Either way, the element outputs combined are analytic signals or, in practice, baseband signals obtained by bandpass filtering and demodulating with a shared complex exponential.

If element outputs have form (23) with element i having pattern $\vec{P}^{\,i}(\boldsymbol{\kappa})$ and array weight w_i, the array output becomes

$$\begin{aligned}\sum_i w_i \int \vec{E}(\boldsymbol{\kappa})\vec{P}^{\,i}(\boldsymbol{\kappa})\,d\boldsymbol{\kappa} = &\int E_{\widehat{\phi}}(\boldsymbol{\kappa})\Big(\sum_i w_i P^i_{\widehat{\phi}}(\boldsymbol{\kappa})\Big)\,d\boldsymbol{\kappa} \\ &+ \int E_{\widehat{\theta}}(\boldsymbol{\kappa})\Big(\sum_i w_i P^i_{\widehat{\theta}}(\boldsymbol{\kappa})\Big)\,d\boldsymbol{\kappa}.\end{aligned} \tag{24}$$

Comparing to (23), we interpret the sums in large parentheses as horizontally and vertically polarized array patterns.

2.1.2 Positioning an Antenna on the Cylinder

Here we consider antenna rotation as well as translation and then specialize to translations along and rotations about the eventual cylindrical array's axis.

Antenna Rotation

Using dimensionless real 3×3 rotation (and hence orthogonal) matrix $\mathbf{R}$, change of variable $\boldsymbol{\kappa}' \triangleq \boldsymbol{\kappa}\mathbf{R}^{-1}$ in (20) yields, once we drop the primes,

$$\mathrm{A}(\mathbf{x}) = \int \vec{E}(\boldsymbol{\kappa}\mathbf{R})\mathbf{R}^{-1}\,\mathbf{R}\vec{P}(\boldsymbol{\kappa}\mathbf{R})\,\mathrm{e}^{\,j2\pi\boldsymbol{\kappa}\mathbf{R}\mathbf{x}}\,d\boldsymbol{\kappa}.$$

Here rotating row vector $\vec{E}(\boldsymbol{\kappa})$ identically in $\boldsymbol{\kappa}$ dependence and as a field vector yields $\vec{E}(\boldsymbol{\kappa}\mathbf{R})\mathbf{R}^{-1}$, and similarly rotating the column-vector pattern of the shifted antenna yields $\mathbf{R}\vec{P}(\boldsymbol{\kappa}\mathbf{R})\,\mathrm{e}^{\,j2\pi\boldsymbol{\kappa}\mathbf{R}\mathbf{x}}$. Each transformation just rotates the spatial coordinate system, and the antenna output is unchanged.

We will soon rotate the antenna and so its pattern without rotating the incident field. Per the above then, define a shifted then rotated pattern, distinguished by its three arguments, as

$$\vec{P}(\boldsymbol{\kappa}, \mathbf{R}, \mathbf{x}) \triangleq \mathbf{R}\vec{P}(\boldsymbol{\kappa}\mathbf{R})\,\mathrm{e}^{\,j2\pi\boldsymbol{\kappa}\mathbf{R}\mathbf{x}}\,. \tag{25}$$

Decomposition of shifted, rotated pattern (25) as in (21) and (22) yields, after (22) is used again to simplify notation,

$$\begin{aligned}
\vec{P}(\boldsymbol{\kappa}, \mathbf{R}, \mathbf{x}) &= P_{\widehat{\phi}}(\boldsymbol{\kappa}, \mathbf{R}, \mathbf{x})\,\widehat{\phi}^{\,T} + P_{\widehat{\theta}}(\boldsymbol{\kappa}, \mathbf{R}, \mathbf{x})\,\widehat{\theta}^{\,T} \\
P_{\widehat{\phi}}(\boldsymbol{\kappa}, \mathbf{R}, \mathbf{x}) &\triangleq \widehat{\phi}\,\mathbf{R}\vec{P}(\boldsymbol{\kappa}\mathbf{R})\,\mathrm{e}^{\,j2\pi\boldsymbol{\kappa}\mathbf{R}\mathbf{x}} = P_{\widehat{\phi}\mathbf{R}}(\boldsymbol{\kappa}\mathbf{R})\,\mathrm{e}^{\,j2\pi\boldsymbol{\kappa}\mathbf{R}\mathbf{x}} \qquad (26) \\
P_{\widehat{\theta}}(\boldsymbol{\kappa}, \mathbf{R}, \mathbf{x}) &\triangleq \widehat{\theta}\,\mathbf{R}\vec{P}(\boldsymbol{\kappa}\mathbf{R})\,\mathrm{e}^{\,j2\pi\boldsymbol{\kappa}\mathbf{R}\mathbf{x}} = P_{\widehat{\theta}\mathbf{R}}(\boldsymbol{\kappa}\mathbf{R})\,\mathrm{e}^{\,j2\pi\boldsymbol{\kappa}\mathbf{R}\mathbf{x}}\,. \qquad (27)
\end{aligned}$$

Subscripts are unit-vector-valued variables, not just text labels.

Express $\boldsymbol{\kappa}$ in a New Coordinate System

Let column vector $\widehat{z}$ be the dimensionless vertical unit vector. Then $P_{\widehat{\phi}}(\boldsymbol{\kappa})$ and $P_{\widehat{\theta}}(\boldsymbol{\kappa})$ of (21) can be written as functions of ϕ and $\kappa_z \triangleq \boldsymbol{\kappa}\widehat{z} = \sin(\theta)/\lambda$, with $r = 1/\lambda$ assumed as before. Vertical component κ_z of look vector $\boldsymbol{\kappa}$ has inverse-length units so is not a height, so we arbitrarily name it the *look vertical*. With left subscripts now text labels rather than variables, define

$$\begin{aligned}
P_{\phi}(\phi, \kappa_z) &\triangleq P_{\widehat{\phi}}(\boldsymbol{\kappa}) \\
P_{\theta}(\phi, \kappa_z) &\triangleq P_{\widehat{\theta}}(\boldsymbol{\kappa}).
\end{aligned} \tag{28}$$

Arguments ϕ and κ_z on the left are the azimuth and look vertical of the look-vector argument on the right. Text subscripts ϕ and θ on the left denote *horizontal and vertical polarization* and flag that the subscripts on the right are the increasing-az and -el unit vectors of the look-vector argument on the right.

Shift Along and Rotate About the Vertical

Cylindrical-array patterns below use vertical shifts $\mathbf{x}_\uparrow$ and matrices $\mathbf{R}$ that rotate about $\mathbf{x}_\uparrow$ for $\mathbf{R}\mathbf{x}_\uparrow = \mathbf{x}_\uparrow$ with $\phi - \varphi$ the azimuth of $\boldsymbol{\kappa}\mathbf{R}$. Then (26) and (27) become, in notation (28) with $\widehat{\phi}\mathbf{R}$ and $\widehat{\theta}\mathbf{R}$ the increasing-azimuth and -elevation unit vectors for $\boldsymbol{\kappa}\mathbf{R}$,

$$\begin{aligned} P_{\widehat{\phi}}(\boldsymbol{\kappa}, \mathbf{R}, \mathbf{x}_\uparrow) &= P_\phi(\phi - \varphi, \kappa_z)\, \mathrm{e}^{\,j2\pi\boldsymbol{\kappa}\mathbf{x}_\uparrow} \\ P_{\widehat{\theta}}(\boldsymbol{\kappa}, \mathbf{R}, \mathbf{x}_\uparrow) &= P_\theta(\phi - \varphi, \kappa_z)\, \mathrm{e}^{\,j2\pi\boldsymbol{\kappa}\mathbf{x}_\uparrow}. \end{aligned} \tag{29}$$

2.1.3 Locate Array Elements on a Wrapped Lattice

Let $\mathbb{Z}^D$ and $\mathbb{Z}^D$ denote respectively the sets of all column and row integer vectors of length D. Of special interest are $\mathbb{Z}^2$ and $\mathbb{Z}^2$, the sets of all integer column and row two-vectors.

Suppose our cylindrical array has its central axis along $\widehat{z}$, has one element's output connected to a receiver, and has each of its other element outputs terminated in an impedance identical to that of the receiver input. Let the *prototype element patterns* of the one active output take form (29) with $\varphi = 0$ and $\mathbf{x}_\uparrow = 0$. The geometry of that one element, including location, is incorporated into $P_\phi(\phi, \kappa_z)$ and $P_\theta(\phi, \kappa_z)$ and need not be represented explicitly, but suppose that physically all elements lie at nominal cylinder radius d, which will become a convenient normalization constant later.

Now imagine a set of arrays created by rotating and shifting the original array by various φ and $\mathbf{x}_\uparrow$ values to place its one active element into each original element's position in turn. If the $(\varphi, \mathbf{x}_\uparrow)$ pairs and the original array's element hardware are both suitably periodic, these new arrays will be identical to the original except with their single outputs taken from different elements. The elements will share common prototype patterns $P_\phi(\phi, \kappa_z)$ and $P_\theta(\phi, \kappa_z)$ in (29) but will have individual shifts φ and $\mathbf{x}_\uparrow$ to create embedded complex *element patterns* at specific array locations. To effectively obtain the outputs of all of the new arrays simultaneously, we use only the original periodic array but with outputs taken from each element using identical receivers. We can't realize the implied infinite vertical extent, but if we realize enough terminated "guard elements" above and below those actually driving receivers, the outputs actually used will behave as if the realized array is periodic.

To obtain the required periodicity, let us index elements on $\boldsymbol{n} \in \mathbb{Z}^2$ with associated rotation φ and shift $\mathbf{x}_\uparrow = z\,\widehat{z}$ set by

$$\begin{pmatrix} \varphi/2\pi \\ z/d \end{pmatrix} = \mathbf{B}\boldsymbol{n} = \begin{pmatrix} \mathbf{b}_1 \\ \mathbf{b}_2 \end{pmatrix} \begin{pmatrix} n_1 \\ n_2 \end{pmatrix} \tag{30}$$

as illustrated by the Fig. 1 dots. Normalizing z by arbitrary scaling length d, fixed above to the nominal cylinder radius, makes $\mathbf{b}_2$ dimensionless like $\mathbf{b}_1$, so that those two real row two-vectors combine into a real 2×2 matrix $\mathbf{B}$. The 2π is just a convenience. If we obtain element pattern $\boldsymbol{n}$ as (29) with rotation matrix $\mathbf{R}$ and shift vector $\mathbf{x}_\uparrow$ subscripted just this once with element index $\boldsymbol{n}$, the horizontally polarized element pattern has $\varphi = 2\pi\mathbf{b}_1\boldsymbol{n}$ and $\boldsymbol{\kappa}\mathbf{x}_\uparrow = \boldsymbol{\kappa}\widehat{z}z = \kappa_z d\,\mathbf{b}_2\boldsymbol{n}$ and is just

$$P_\phi(\phi - 2\pi\mathbf{b}_1\boldsymbol{n}, \kappa_z)\, \mathrm{e}^{\,j2\pi\kappa_z d\mathbf{b}_2\boldsymbol{n}}\,. \tag{31}$$

From here onward we show results for horizontal polarization. Vertical polarization is the same but with subscript $\widehat{\theta}$ instead.

The needed periodicity requires an *index period* $\boldsymbol{p} \in \mathbb{Z}^2$ with

$$\mathbf{B}\boldsymbol{p} = \begin{pmatrix} 1 \\ 0 \end{pmatrix}. \tag{32}$$

Incrementing $\boldsymbol{n}$ by $\boldsymbol{p}$ in (30) increments φ by 2π without disturbing z. Element coordinates $\binom{\varphi/2\pi}{z/d}$ of form $\mathbf{B}\boldsymbol{n}$ comprise a point lattice wrapped around a cylinder of unit circumference, with the columns of basis matrix $\mathbf{B}$ as lattice basis vectors.

Remember that the prototype pattern represents an element embedded in the array, not one physically located at the origin. This embedding sweeps mutual coupling into the prototype pattern so that it need not be represented explicitly.

Use Coset Decomposition for Finitely Many Elements

In the coordinates of (30), element $\boldsymbol{n}$ has the nominal position $\mathbf{B}\boldsymbol{n}$. Ranging $\boldsymbol{n}$ over $\mathbb{Z}^2$ yields the infinitely many positions of lattice $\mathbf{B}\mathbb{Z}^2$, for example the Fig. 1 dots continued indefinitely in all directions. Now we will partition the plane into identical tiles that tile the plane and then populate the array, exclusive of guard elements, at only a single tile's lattice points. First we concisely present a few needed basics of lattices, sublattices, coset decomposition, and associated notation, but see [7] for a more thorough and less terse presentation of those ideas.

A rectangular tile will suffice here, though it is not required for lattice work in general. Construct it with $\boldsymbol{p} \in \mathbb{Z}^2$ of (32) and any nonzero $\boldsymbol{q} \in \mathbb{Z}^2$ with $\mathbf{B}\boldsymbol{p} \perp \mathbf{B}\boldsymbol{q}$ (needed later for the phase-mode pattern sum in Section 2.1.4) as shown by the thin dark lines in Fig. 1. Give the *fundamental tile* corners 0, $\mathbf{B}\boldsymbol{p}$, $\mathbf{B}\boldsymbol{q}$, and $\mathbf{B}(\boldsymbol{p}+\boldsymbol{q})$ and contain its interior, the origin, and the two sides that have the origin as one endpoint. To tile the plane, *i.e.* partition the plane into tiles, translate this fundamental tile by integer combinations of corners $\mathbf{B}\boldsymbol{p}$ and $\mathbf{B}\boldsymbol{q}$, that is by $\mathbf{BN}\boldsymbol{n}'$ where $\boldsymbol{n}' \in \mathbb{Z}^2$ and

$$\mathbf{N} \triangleq (\boldsymbol{p}, \boldsymbol{q}). \tag{33}$$

As an invertible integer matrix, $\mathbf{N}$ is a *resampling matrix*. The set of $\mathbf{BN}\boldsymbol{n}'$ for $\boldsymbol{n}' \in \mathbb{Z}^2$ is sublattice $\mathbf{BN}\mathbb{Z}^2 \subset \mathbf{B}\mathbb{Z}^2$ with basis matrix $\mathbf{BN}$. Likewise, lattice $\mathbb{Z}^2$ has basis matrix $\mathbf{I}$, the identity, and has sublattice $\mathbf{N}\mathbb{Z}^2 \subset \mathbb{Z}^2$ with basis matrix $\mathbf{N}$.

The same tiles partition lattice $\mathbf{B}\mathbb{Z}^2$ into disjoint subsets of $|\mathbf{N}|$ points each, 24 points per tile in Fig. 1, because [7, Section 2.3.1] the ratio of the density of lattice $\mathbf{B}\mathbb{Z}^2$ to the density of sublattice $\mathbf{BN}\mathbb{Z}^2$ is $|\mathbf{N}|$, short for $|\det(\mathbf{N})|$. For any $\boldsymbol{n} \in \mathbb{Z}^2$, there is one combination of $\boldsymbol{n}_\square \in \mathbb{Z}^2$ and $\boldsymbol{n}' \in \mathbb{Z}^2$ that yields *coset decomposition* $\mathbf{B}\boldsymbol{n} = \mathbf{B}\boldsymbol{n}_\square + \mathbf{BN}\boldsymbol{n}'$ with $\mathbf{B}\boldsymbol{n}_\square$ the position of a lattice point in the fundamental tile and $\mathbf{BN}\boldsymbol{n}'$ a tile's translation. Corresponding coset decomposition $\boldsymbol{n} = \boldsymbol{n}_\square + \mathbf{N}\boldsymbol{n}'$, of course also unique, is implied and defines $\boldsymbol{n} \bmod \mathbf{N} \triangleq \boldsymbol{n}_\square$, just as for the usual integer relationships. Notation $\left[\mathbb{Z}^2/\mathbf{N}\mathbb{Z}^2\right]$ from elementary group theory [8, 9] here denotes the set of $|\mathbf{N}|$ allowed $\boldsymbol{n}_\square$ values, the remainders returned by the $\bmod$ operation and that put $\mathbf{B}\boldsymbol{n}_\square$ in the fundamental tile. Notation $\left[\mathbb{Z}^2/\mathbf{N}\mathbb{Z}^2\right]$ refers to lattice $\mathbb{Z}^2$ and

sublattice $\mathbf{N}\mathbb{Z}^2$ from which $\boldsymbol{n}$ and $\mathbf{N}\boldsymbol{n}'$ are respectively drawn in coset decomposition $\boldsymbol{n} = \boldsymbol{n}_\square + \mathbf{N}\boldsymbol{n}'$. Likewise, $\left[\mathbf{B}\mathbb{Z}^2/\mathbf{B}\mathbf{N}\mathbb{Z}^2\right]$ denotes the points of $\mathbf{B}\mathbb{Z}^2$ in a tile, but we will not actually need that notation.

We can generalize on the tiling construction by partitioning $\mathbb{Z}^2$ into subsets with one subset denoted by $\left[\mathbb{Z}^2/\mathbf{N}\mathbb{Z}^2\right]$ and with each other subset just $\left[\mathbb{Z}^2/\mathbf{N}\mathbb{Z}^2\right]$ offset by an element of $\mathbf{N}\mathbb{Z}^2$. A partition comprises disjoint subsets, so $\left[\mathbb{Z}^2/\mathbf{N}\mathbb{Z}^2\right]$ can contain no two indices having their difference in $\mathbf{N}\mathbb{Z}^2$. This generality allows us to start with one partitioning, perhaps using tiles, and derive another by individually translating indices in the original $\left[\mathbb{Z}^2/\mathbf{N}\mathbb{Z}^2\right]$ by arbitrary points of sublattice $\mathbf{B}\mathbf{N}\mathbb{Z}^2$. In fact the indices in any choice of $\left[\mathbb{Z}^2/\mathbf{N}\mathbb{Z}^2\right]$ will be related to the original tile-based $\left[\mathbb{Z}^2/\mathbf{N}\mathbb{Z}^2\right]$ by individual offsets from $\mathbf{N}\mathbb{Z}^2$ in just that way, so if we use tile geometry to compute $\boldsymbol{n} \bmod \mathbf{N}$ for the original $\left[\mathbb{Z}^2/\mathbf{N}\mathbb{Z}^2\right]$, say with the procedure of [7, Sections 5.3.1 through 5.3.4], we can obtain $\boldsymbol{n} \bmod \mathbf{N}$ for the new $\left[\mathbb{Z}^2/\mathbf{N}\mathbb{Z}^2\right]$ by adding the appropriate offset, perhaps obtained from a lookup table. In Fig. 1 for example, we could include the lower starred point rather than the upper starred point in the modified tile.

Such point offsets can, in aggregate, even modify the fundamental tile in the original construction by rotation, reflection, or translation (thick lines in Fig. 1). If desired we can even translate individual tile points further afterward, again by points in $\mathbf{N}\mathbb{Z}^2$, before we finally denote the indices of its lattice points by $\left[\mathbb{Z}^2/\mathbf{N}\mathbb{Z}^2\right]$. All these options effectively move or bend tile boundaries but with the plane still tiled.

The $\left[\mathbb{Z}^2/\mathbf{N}\mathbb{Z}^2\right]$ notation misleads by suggesting that "/" and "[ ]" are computational operations, but instead $\left[\mathbb{Z}^2/\mathbf{N}\mathbb{Z}^2\right]$ as a unit denotes any subset of $\mathbb{Z}^2$ chosen such that its translations by offsets in sublattice $\mathbf{N}\mathbb{Z}^2 \subset \mathbb{Z}^2$ exactly partition $\mathbb{Z}^2$. Once $\left[\mathbb{Z}^2/\mathbf{N}\mathbb{Z}^2\right]$ is chosen though, it is fixed, not variable.

The Appendix will use certain group-theoretic properties of $\left[\mathbb{Z}^2/\mathbf{N}\mathbb{Z}^2\right]$, but here it is enough that we have chosen $\mathbf{B}\mathbb{Z}^2$ and $\mathbf{N} = (\boldsymbol{p}, \boldsymbol{q})$ and constructed $\left[\mathbb{Z}^2/\mathbf{N}\mathbb{Z}^2\right]$ so that the desired element locations are $\mathbf{B}\boldsymbol{n}$ for $\boldsymbol{n} \in \left[\mathbb{Z}^2/\mathbf{N}\mathbb{Z}^2\right]$.

We also uniquely decompose row vector $\boldsymbol{m} \in \mathbb{Z}^2$ below as $\boldsymbol{m} = \boldsymbol{m}_\square + \boldsymbol{m}'\mathbf{N}$ with $\boldsymbol{m}' \in \mathbb{Z}^2$ and $\boldsymbol{m}_\square \in \left[\mathbb{Z}^2/\mathbb{Z}^2\mathbf{N}\right]$, but $\left[\mathbb{Z}^2/\mathbb{Z}^2\mathbf{N}\right]$ will be arbitrary and not involve element positions.

We'll use sums like $\boldsymbol{n}_\square + \mathbf{N}\boldsymbol{n}'$ and $\boldsymbol{m}_\square + \boldsymbol{m}'\mathbf{N}$ heavily below, but we'll not use the awkward variable names $\boldsymbol{n}_\square$ and $\boldsymbol{m}_\square$. Instead we'll generally call the latter just $\boldsymbol{n}$ and $\boldsymbol{m}$.

2.1.4 The Array Pattern's Several Basic Forms

Below we develop four distinct forms of the array pattern. All except the last are developed in this section and depend on a continuous elevation parameter. The last, developed in the next section, depends on a discretized elevation.

A. Form (37) below is a weighted sum of element patterns.
B. Form (43) is a weighted sum of *phase-mode* patterns.

We will see that the phase-mode patterns and weights relate to the element patterns and and weights through a generalized discrete Fourier transform (DFT). A Fourier series in azimuth for the prototype element pattern then yields two more forms.

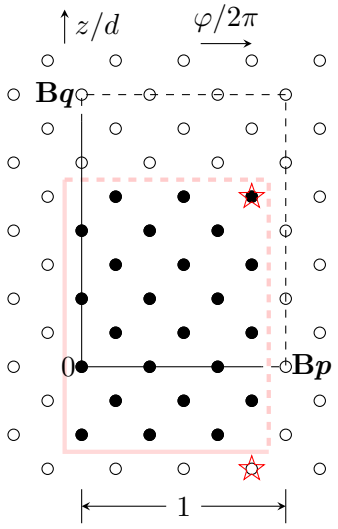

Fig. 1 — Construct nominal weight locations (filled dots) in the $\left(\frac{\varphi/2\pi}{z/d}\right)$ plane using lattice basis matrix $\mathbf{B}$, index period $\boldsymbol{p} \in \mathbb{Z}^2$, and some $\boldsymbol{q} \in \mathbb{Z}^2$ with $\mathbf{B}\boldsymbol{p} \perp \mathbf{B}\boldsymbol{q}$ to construct a semi-open rectangle, optionally rotate, reflect, and/or translate it arbitrarily, identify the contained points of the lattice $\mathbf{B}\mathbb{Z}^2$, and optionally offset each by any point of sublattice $\mathbf{B}\mathbf{N}\mathbb{Z}^2$, where resampling matrix $\mathbf{N} = (\boldsymbol{p}, \boldsymbol{q})$. (Example: fill the lower star instead of the upper star.) The locations obtained take form $\mathbf{B}\boldsymbol{n}$ with $\boldsymbol{n} \in \left[\mathbb{Z}^2/\mathbf{N}\mathbb{Z}^2\right]$.

C. Form (39) is an azimuth Fourier series that is based on a generalized discrete-time Fourier transform (DTFT) of the weights from A above.
D. Form (47) is an azimuth Fourier series using phase-mode weights and a discretized elevation parameter.

Form A is often used for pattern optimization. Then B, derived from it, supports computing embedded element patterns using unit cells [10]. Azimuth Fourier-series form C discretized in elevation becomes D, and both forms offer insights into array parameter selection [4]. With zero padding (zero-weighted extra elements) D can be useful for computing samples of C for plotting (When is this true? Both C and D require elt patt FS coeffs at every elevation of interest.) and also leads below to relatively simple if suboptimal azimuth steering. (Optimal steering instead reoptimizes the array pattern for each pointing direction.)

A Fourier-Series Prototype Element Pattern

In element pattern (31), the element's height offset appears in a complex exponential, and a Fourier series will allow its azimuth offset to do so also, with their combined exponent a matrix bilinear form. This generalizes an approach of Taylor [1] that led him, for uniform circular arrays (UCAs), to the classic phase-mode formulation and associated azimuth-steering approach [2, 4], just as our generalization will do here for cylindrical arrays.

To begin, write the prototype element pattern as an exponential Fourier series—the sum is doubly infinite—in azimuth,

$$P_\phi(\phi, \kappa_z) = \sum_k a_k(\kappa_z)\, \mathrm{e}^{jk\phi}\,. \tag{34}$$

Taking (31) as the element pattern of array element $\boldsymbol{n}$,

$$P_{\boldsymbol{n}}(\phi,\kappa_z) \triangleq P_{\phi}(\phi - 2\pi\mathbf{b}_1\boldsymbol{n},\kappa_z)\,\mathrm{e}^{\,j2\pi\kappa_z d\mathbf{b}_2\boldsymbol{n}}\,. \tag{35}$$

On the right use Fourier series (34) and basis definition (30),

$$\begin{aligned} P_{\boldsymbol{n}}(\phi,\kappa_z) &= \sum_k a_k(\kappa_z)\,\mathrm{e}^{-j2\pi(k\mathbf{b}_1-\kappa_z d\mathbf{b}_2)\boldsymbol{n}}\,\mathrm{e}^{\,jk\phi} \\ &= \sum_k a_k(\kappa_z)\,\mathrm{e}^{-j2\pi(k,-\kappa_z d)\mathbf{B}\boldsymbol{n}}\,\mathrm{e}^{\,jk\phi}\,. \end{aligned} \tag{36}$$

Ordinary Array-Pattern Sum

As in (24), the array pattern is a weighted sum of element patterns, but here the sum uses only the finite number of elements indexed by $\boldsymbol{n} \in \left[\mathbb{Z}^2/\mathbf{N}\mathbb{Z}^2\right]$ as developed in Section 2.1.3. The array pattern then has form

$$C(\phi,\kappa_z) \triangleq \sum_{\boldsymbol{n}\in[\mathbb{Z}^2/\mathbf{N}\mathbb{Z}^2]} w_{\boldsymbol{n}} P_{\boldsymbol{n}}(\phi,\kappa_z) \tag{37}$$

$$= \sum_k a_k(\kappa_z) \sum_{\boldsymbol{n}\in[\mathbb{Z}^2/\mathbf{N}\mathbb{Z}^2]} w_{\boldsymbol{n}}\,\mathrm{e}^{-j2\pi(k,-\kappa_z d)\mathbf{B}\boldsymbol{n}}\,\mathrm{e}^{\,jk\phi} \tag{38}$$

$$= \sum_k a_k(\kappa_z)\, W\big((k,-\kappa_z d)\mathbf{B}\big)\,\mathrm{e}^{\,jk\phi} \tag{39}$$

using (36) in (38). Here (39) uses a function of real row two-vector $\boldsymbol{f}$ that generalizes a 2D DTFT of element weights $w_{\boldsymbol{n}}$:

$$W(\boldsymbol{f}) \triangleq \sum_{\boldsymbol{n}\in[\mathbb{Z}^2/\mathbf{N}\mathbb{Z}^2]} w_{\boldsymbol{n}}\,\mathrm{e}^{-j2\pi\boldsymbol{f}\boldsymbol{n}}\,. \tag{40}$$

The generalization is in the indices of summation used.

Phase-Mode Pattern Sum

Yet another Fourier domain yields an alternative to (37) and (39). Apply a generalized DFT [7] to the element outputs to obtain $|\mathbf{N}|$ *phase-mode* outputs with the $\boldsymbol{m}$th having phase-mode pattern, for $\boldsymbol{m} \in \left[\mathbb{Z}^2/\mathbb{Z}^2\mathbf{N}\right]$,

$$Y_{\boldsymbol{m}}(\phi,\kappa_z) \triangleq \sum_{\boldsymbol{n}\in[\mathbb{Z}^2/\mathbf{N}\mathbb{Z}^2]} P_{\boldsymbol{n}}(\phi,\kappa_z)\,\mathrm{e}^{-j2\pi\boldsymbol{m}\mathbf{N}^{-1}\boldsymbol{n}}\,. \tag{41}$$

We can likewise transform the weights to define

$$W_{\boldsymbol{m}} \triangleq \sum_{\boldsymbol{n}\in[\mathbb{Z}^2/\mathbf{N}\mathbb{Z}^2]} w_{\boldsymbol{n}}\,\mathrm{e}^{-j2\pi\boldsymbol{m}\mathbf{N}^{-1}\boldsymbol{n}}\,. \tag{42}$$

Definitions (41) and (42) of $Y_{\boldsymbol{m}}(\phi, \kappa_z)$ and $W_{\boldsymbol{m}}$ easily extend periodically to $\boldsymbol{m} \in \mathbb{Z}^2$ with a period comprising $\left[\mathbb{Z}^2/\mathbb{Z}^2\mathbf{N}\right]$. We just use coset decomposition $\boldsymbol{m} = (\boldsymbol{m} \bmod \mathbf{N}) + \boldsymbol{m}'\mathbf{N}$ to replace index $\boldsymbol{m}$ on the right with $\boldsymbol{m} \bmod \mathbf{N} \in \left[\mathbb{Z}^2/\mathbb{Z}^2\mathbf{N}\right]$. The exponential's periodicity makes $\boldsymbol{m}'\mathbf{N}$ irrelevant for every $\boldsymbol{m}' \in \mathbb{Z}^2$.

Applying the inverse DFT from the Appendix to (41),

$$P_{\boldsymbol{n}}(\phi, \kappa_z) = \frac{1}{|\mathbf{N}|} \sum_{\boldsymbol{m} \in [\mathbb{Z}^2/\mathbb{Z}^2\mathbf{N}]} Y_{\boldsymbol{m}}(\phi, \kappa_z)\, \mathrm{e}^{\,j2\pi \boldsymbol{m}\mathbf{N}^{-1}\boldsymbol{n}}$$

which in (37) yields, after a little reordering,

$$C(\phi, \kappa_z) = |\mathbf{N}|^{-1} \sum_{\boldsymbol{m} \in [\mathbb{Z}^2/\mathbb{Z}^2\mathbf{N}]} \Big(\sum_{\boldsymbol{n} \in [\mathbb{Z}^2/\mathbf{N}\mathbb{Z}^2]} w_{\boldsymbol{n}}\, \mathrm{e}^{\,j2\pi \boldsymbol{m}\mathbf{N}^{-1}\boldsymbol{n}} \Big) Y_{\boldsymbol{m}}(\phi, \kappa_z).$$

Using DFT (42) to rewrite the contents of the parentheses,

$$C(\phi, \kappa_z) = \frac{1}{|\mathbf{N}|} \sum_{\boldsymbol{m} \in [\mathbb{Z}^2/\mathbb{Z}^2\mathbf{N}]} W_{-\boldsymbol{m}} Y_{\boldsymbol{m}}(\phi, \kappa_z). \tag{43}$$

Computationally, subscript $-\boldsymbol{m}$ can be reduced modulo $\mathbf{N}$. Change of basis (41) and (42) relates the equivalent weighted array-pattern sums here and in (37), and the next section will further relate these array-pattern sums through the sampling relationship $W_{\boldsymbol{m}} = W(\boldsymbol{m}\mathbf{N}^{-1})$ that connects (40) and (42).

2.1.5 Simple, Approximate Steering

Our simple approach to azimuth steering generalizes [4], a modern presentation of an approach of Sheleg [2]. Unlike that earlier UCA work, the generalization here to cylindrical arrays, curiously, requires discretizing the look vertical κ_z.

Discretizing κ_z

Ideally, azimuth steering by ϕ_s would replace ϕ with $\phi - \phi_s$ in array pattern $C(\phi, \kappa_z)$. Can this be done by modifying weights? Replacement in array sum (37) or (43) physically rotates the array by ϕ_s, which is not helpful, and in (38) it scales $w_{\boldsymbol{n}}$ by an exponential dependent, unacceptably, on Fourier-series index k. Is the steered pattern even in the space realizable by the sums of (37) and (43)? No. They have only $|\mathbf{N}|$ degrees of freedom. We must approximate.

Our steering approximation will use a version of $C(\phi, \kappa_z)$ discretized in κ_z, push the ϕ_s dependence into Fourier phase-mode factor $\mathrm{e}^{\,jk\phi}$ for the largest Fourier terms, and then simply ignore the distortion this introduces into the smaller terms.

First discretize in κ_z. Definitions (30) and (33) of $\mathbf{B}$ and $\mathbf{N}$, index periodicity (32), and orthogonality $\mathbf{B}\boldsymbol{p} \perp \mathbf{B}\boldsymbol{q}$ imply

$$\mathbf{BN} = \mathbf{B}\big(\boldsymbol{p}, \boldsymbol{q}\big) = \big(\mathbf{B}\boldsymbol{p}, \mathbf{B}\boldsymbol{q}\big) = \begin{pmatrix} 1 & 0 \\ 0 & z_q/d \end{pmatrix}$$

where z_q/d is the vertical extent of the original tiling rectangle in Fig. 1. So with an eye toward replacing the DTFT in array pattern (39) with DFT coefficients, we discretize look vertical κ_z in (38) to obtain $(k, -\kappa_z d)\mathbf{B} = \boldsymbol{\ell}\mathbf{N}^{-1}$ for $\boldsymbol{\ell} \in \mathbb{Z}^2$ by setting

$$\begin{aligned} \boldsymbol{\ell} &= (k, -\kappa_z d)\mathbf{B}\mathbf{N} && (44) \\ &= (k, -\kappa_z d) \begin{pmatrix} 1 & 0 \\ 0 & z_q/d \end{pmatrix} \\ &= (k, -\kappa_z z_q). && (45) \end{aligned}$$

Only finitely many of the discretized $\kappa_z = -\ell_2/z_q$ are relevant, because of Helmholtz relation $-1/\lambda \leq \kappa_z \leq 1/\lambda$. Discretization (44) and weight DFT (42) in (38) yield

$$\begin{aligned} C(\phi, \kappa_z) &= \sum_k a_{\boldsymbol{\ell}} W_{\boldsymbol{\ell}} \, \mathrm{e}^{jk\phi} && (46) \\ &= \sum_k a_{\boldsymbol{\ell}} W_{\boldsymbol{\ell} \bmod \mathbf{N}} \, \mathrm{e}^{jk\phi} && (47) \end{aligned}$$

where we have written $a_k(\kappa_z)$ as $a_{\boldsymbol{\ell}}$, with row two-vector index $\boldsymbol{\ell} \in \mathbb{Z}^2$ emphasing that κ_z is now discrete. Alternate form (47) emphasizes the periodicity of $W_{\boldsymbol{\ell}}$. Hereafter we must also remember, per (45), that $\boldsymbol{\ell}$ in (46) and (47) depends on k.

Azimuth Steering

At our discrete κ_z, replacing ϕ with $\phi - \phi_s$ in (46) yields the ideally steered array pattern

$$C(\phi - \phi_s, \kappa_z) = \sum_k a_{\boldsymbol{\ell}} \, \mathrm{e}^{-jk\phi_s} \, W_{\boldsymbol{\ell}} \, \mathrm{e}^{jk\phi} \, . \tag{48}$$

Replacing Fourier coefficients $a_{\boldsymbol{\ell}}$ with $a_{\boldsymbol{\ell}} \, \mathrm{e}^{-jk\phi_s}$ would rotate the element pattern, and indeed the array, by ϕ_s. Here we will approximate that impractical ideal with modified Fourier series

$$C(\phi - \phi_s, \kappa_z) \approx \sum_k a_{\boldsymbol{\ell}} \, S_{\boldsymbol{\ell}} \, W_{\boldsymbol{\ell}} \, \mathrm{e}^{jk\phi} \tag{49}$$

with new quantity $S_{\boldsymbol{\ell}}$ of the same period as $W_{\boldsymbol{\ell}}$. In implementation then, $W_{\boldsymbol{\ell}}$ in phase-mode pattern sum (43) or the corresponding real-time beamsum can be replaced with product $S_{\boldsymbol{\ell}} W_{\boldsymbol{\ell}}$. Alternatively, weights $w_{\boldsymbol{n}}$ in original pattern sum (37) and the corresponding beamsums in large parentheses in (24) can be replaced with steered weights $w'_{\boldsymbol{n}}$ computed using the inverse, (A2) in the Appendix, of DFT (42):

$$w'_{\boldsymbol{n}} \triangleq \frac{1}{|\mathbf{N}|} \sum_{\boldsymbol{m} \in [\mathbb{Z}^2/\mathbb{Z}^2\mathbf{N}]} S_{\boldsymbol{m}} W_{\boldsymbol{m}} \, \mathrm{e}^{j2\pi \boldsymbol{m}\mathbf{N}^{-1}\boldsymbol{n}} \, .$$

In any of these approaches, steering phase factor $S_{\boldsymbol{\ell}}$ is set to the correct phase factor $\mathrm{e}^{-jk\phi_s}$ for the $|\mathbf{N}|$ values of $\boldsymbol{\ell}$ in one carefully chosen period of $W_{\boldsymbol{\ell}}$. For other $\boldsymbol{\ell}$, periodicity determines $S_{\boldsymbol{\ell}}$, and the pattern

distortion that stems from having the "wrong" steering phase factors is simply accepted. The significance of this distortion and design strategies to mitigate it are appropriate future research topics.

Before choosing a period in $\boldsymbol{\ell}$ over which to ideally steer $W_{\boldsymbol{\ell}}$, let us examine the periodicity of $W_{\boldsymbol{\ell}}$ in (46). In unique coset decomposition $\boldsymbol{\ell} = \boldsymbol{m} + \boldsymbol{m}'\mathbf{N}$, we usually suppose that $\boldsymbol{m}' \in \mathbb{Z}^2$ and $\boldsymbol{m} \in \left[\mathbb{Z}^2/\mathbb{Z}^2\mathbf{N}\right]$ respectively select a period and an intra-period position. But recall we always had some freedom in choosing set $\left[\mathbb{Z}^2/\mathbb{Z}^2\mathbf{N}\right]$. In fact we can choose an alternate $\left[\mathbb{Z}^2/\mathbb{Z}^2\mathbf{N}\right]$ by adding and subtracting term $\boldsymbol{m}''\mathbf{N}$, for any $\boldsymbol{m}'' \in \mathbb{Z}^2$ we like, to our present coset decomposition:

$$\boldsymbol{\ell} = (\boldsymbol{m} + \boldsymbol{m}''\mathbf{N}) + (\boldsymbol{m}' - \boldsymbol{m}'')\mathbf{N}.$$

If $\boldsymbol{m}$ determines $\boldsymbol{m}''$, the first parentheses contain $|\mathbf{N}|$ possible values that form an alternate choice for $\left[\mathbb{Z}^2/\mathbb{Z}^2\mathbf{N}\right]$, because no two such values, say $\boldsymbol{m}_1 + \boldsymbol{m}_1''\mathbf{N}$ and $\boldsymbol{m}_2 + \boldsymbol{m}_2''\mathbf{N}$, differ by $\boldsymbol{m}_3''\mathbf{N}$ for any $\boldsymbol{m}_3'' \in \mathbb{Z}^2$. To prove it, assume temporarily that

$$(\boldsymbol{m}_1 + \boldsymbol{m}_1''\mathbf{N}) - (\boldsymbol{m}_2 + \boldsymbol{m}_2''\mathbf{N}) = \boldsymbol{m}_3''\mathbf{N}.$$

The standard argument then observes that since this is just

$$\boldsymbol{m}_1 - \boldsymbol{m}_2 = (\boldsymbol{m}_3'' - \boldsymbol{m}_1'' + \boldsymbol{m}_2'')\mathbf{N}$$

it contradicts the definition of $\left[\mathbb{Z}^2/\mathbb{Z}^2\mathbf{N}\right]$, which requires that no two of the latter's elements differ by $\boldsymbol{m}'''\mathbf{N}$ for any $\boldsymbol{m}''' \in \mathbb{Z}^2$. Recall that per definition (42), offsetting the subscript in $W_{\boldsymbol{\ell}}$ by elements of $\mathbb{Z}^2\mathbf{N}$ in this way is completely harmless.

We won't actually choose $\left[\mathbb{Z}^2/\mathbb{Z}^2\mathbf{N}\right]$ again but will simply use the existing $\left[\mathbb{Z}^2/\mathbb{Z}^2\mathbf{N}\right]$ and consider one period of $W_{\boldsymbol{\ell}}$ to be the $|\mathbf{N}|$ values of $\boldsymbol{m} + \boldsymbol{m}'\mathbf{N}$ that have $\boldsymbol{m} \in \left[\mathbb{Z}^2/\mathbb{Z}^2\mathbf{N}\right]$ and that have $\boldsymbol{m}' \in \mathbb{Z}^2$ determined by $\boldsymbol{m}$ in some way. Let us in particular choose $\boldsymbol{m}' \in \mathbb{Z}^2$ to maximize $|a_{\boldsymbol{\ell}} W_{\boldsymbol{\ell}}|$ so that $\boldsymbol{\ell} = \boldsymbol{m} + \boldsymbol{m}'\mathbf{N}$ indexes the largest-magnitude terms in the sum of (46), where largest means over all k and over those κ_z satisfying Helmholtz relation $-1/\lambda \leq \kappa_z \leq 1/\lambda$. This steers terms in this one period in $\boldsymbol{\ell}$ exactly while allowing smaller terms in other periods to suffer phase distortion because their $S_{\boldsymbol{\ell}}$ values are determined by periodicity rather than steering.

To state this formally, for each $\boldsymbol{m} \in \left[\mathbb{Z}^2/\mathbb{Z}^2\mathbf{N}\right]$ let

$$\boldsymbol{m}' \triangleq \operatorname*{argmax}_{m'' \in \mathbb{Z}^2} |a_{\boldsymbol{m}+\boldsymbol{m}''\mathbf{N}} W_{\boldsymbol{m}}|. \tag{50}$$

For any particular $\boldsymbol{m}$ then, steering phase factor $S_{\boldsymbol{\ell}}$ for $\boldsymbol{\ell} = \boldsymbol{m} + \boldsymbol{m}''\mathbf{N}$ is, for any $\boldsymbol{m}'' \in \mathbb{Z}^2$,

$$S_{\boldsymbol{m}+\boldsymbol{m}''\mathbf{N}} \triangleq \mathrm{e}^{-j(m_1 + \boldsymbol{m}'\boldsymbol{p})\phi_s}. \tag{51}$$

Parenthesized quantity $m_1 + \boldsymbol{m}'\boldsymbol{p} = [\boldsymbol{m} + \boldsymbol{m}'\mathbf{N}]_1$. For the correct-phase period where $\boldsymbol{m}'' = \boldsymbol{m}'$, this quantity is just $\boldsymbol{\ell}_1$ or k. For distorted-phase periods, it is determined by periodicity.

REFERENCES

1. T. Taylor, "A synthesis method for circular and cylindrical antennas composed of discrete elements," *Trans. IRE Prof. Group Antennas Propag.*, **PGAP-3**, 251–261, Aug. 1952.

2. B. Sheleg, "A matrix-fed circular array for continuous scanning," *Proc. IEEE*, **56**(11), 2016–2027, Nov. 1968.

3. W. M. Dorsey and A. Stumme, "Simple phase-mode coefficients for equiripple sidelobe reduction from a uniform circular array," in *IEEE Int'l Symp. Antennas and Propag.*, 2018, 2101–2102.

4. J. O. Coleman and W. M. Dorsey, "Phase-Shift Steer a Uniform Circular Array in the Fourier-Series Domain," in *IEEE 18th Wireless and Microwave Technology Conf. (WAMICON)*, Cocoa Beach FL, USA, 24 –25 April 2017.

5. J. O. Coleman, "Signals and systems II—Part III: Analytic signals and QAM data transmission," *IEEE Potentials*, **29**(3), 40–44, May 2010.

6. J. E. Roy and L. Shafai, "Generalization of the Ludwig-3 definition for linear copolarization and cross polarization," *IEEE Trans. Antennas Propag.*, **49**(6), 1006–1010, June 2001.

7. J. O. Coleman, "Planar arrays on lattices and their FFT steering, a primer," Naval Research Laboratory, Washington DC, USA, NRL Formal Report FR/5320--11-10,207, Apr. 29, 2011.

8. I. N. Herstein, *Topics in Algebra*, 2nd ed. (Wiley, NY, 1975).

9. N. Jacobson, *Basic Algebra I*, 2nd ed. (W. H. Freeman, NY, 1985).

10. C. J. Fulton and A. Mirkamali, "A computer-aided technique for the analysis of embedded element patterns of cylindrical arrays [EM Programmer's Notebook]," *IEEE Antennas Propag. Mag.*, **57**(3), 132–138, June 2015.

Appendix

INVERTING THE LATTICE DISCRETE FOURIER TRANSFORM

Here we prove that the DFT and inverse DFT truly invert each other, but in a general lattice setting. Positive integer D is the transform dimension, and $\mathbf{N}$ is a $D \times D$ resampling (invertible, integer) matrix. A diagonal $\mathbf{N}$ makes the general transform pair considered here into an ordinary multidimensional DFT/IDFT pair, and setting $D = 1$ makes $\mathbf{N}$ a scalar so that the transform becomes the standard one-dimensional DFT/IDFT taught to electrical-engineering undergraduates.

We assume reader comfort with coset-decomposition basics. For the special case of 2D lattices, these basics are developed tutorially in [7, Section 2] and summarized in the Section 2.1.3 tile discussion above. We also assume certain basics of cyclic groups and of homomorphism in groups as typically found in early parts of undergraduate abstract-algebra texts [8, 9].

THE TRANSFORM PAIR

Our generalized DFT definition

$$W_{\boldsymbol{k}} = \sum_{\boldsymbol{n} \in [\mathbb{Z}^D / \mathbf{N}\mathbb{Z}^D]} w_{\boldsymbol{n}} \, \mathrm{e}^{-j2\pi \boldsymbol{k} \mathbf{N}^{-1} \boldsymbol{n}} \tag{A1}$$

is defined for "frequency" index vector $\boldsymbol{k} \in \left[\mathbb{Z}^D / \mathbb{Z}^D \mathbf{N}\right]$ but can easily be extended periodically, since replacing $\boldsymbol{k}$ with $\boldsymbol{k} + \boldsymbol{k}' \mathbf{N}$ for any $\boldsymbol{k}' \in \mathbb{Z}^D$ leaves the right side unchanged.

The corresponding inverse-DFT definition

$$w_{\boldsymbol{n}} = \frac{1}{|\mathbf{N}|} \sum_{\boldsymbol{k} \in [\mathbb{Z}^D / \mathbb{Z}^D \mathbf{N}]} W_{\boldsymbol{k}} \, \mathrm{e}^{j2\pi \boldsymbol{k} \mathbf{N}^{-1} \boldsymbol{n}} \tag{A2}$$

is defined for "time" index vector $\boldsymbol{n} \in \left[\mathbb{Z}^D / \mathbf{N}\mathbb{Z}^D\right]$ but can easily be extended periodically, since replacing $\boldsymbol{n}$ with $\boldsymbol{n} + \mathbf{N}\boldsymbol{n}'$ for any $\boldsymbol{n}' \in \mathbb{Z}^D$ leaves the right side unchanged. The structure of (A2) averages the sum's terms, as there are $|\mathbf{N}|$ members in the set $\left[\mathbb{Z}^D / \mathbb{Z}^D \mathbf{N}\right]$ of coset representatives, a fact deriving from the determinant $|\mathbf{N}|$ being, to within a sign, the ratio of the volumes of the unit cells (parallotopes defined by their basis vectors) of lattice $\mathbb{Z}^D$ and sublattice $\mathbb{Z}^D \mathbf{N}$.

THE ESSENCE OF THE DESIRED INVERSION RESULT

Below we prove specifically that the IDFT inverts the DFT. Separately proving that the DFT inverts the IDFT is not necessary, as the two proofs are the same except for minor sign differences.

Let us reduce the required proof to its essence. Substituting DFT (A1) into IDFT (A2) and reordering,

$$\frac{1}{|\mathbf{N}|}\sum_{\boldsymbol{k}\in[\mathbb{Z}^D/\mathbb{Z}^D\mathbf{N}]}\Big(\sum_{\boldsymbol{m}\in[\mathbb{Z}^D/\mathbf{N}\mathbb{Z}^D]} w_{\boldsymbol{m}}\,\mathrm{e}^{-j2\pi\boldsymbol{k}\mathbf{N}^{-1}\boldsymbol{m}}\Big)\,\mathrm{e}^{j2\pi\boldsymbol{k}\mathbf{N}^{-1}\boldsymbol{n}} = \sum_{\boldsymbol{m}\in[\mathbb{Z}^D/\mathbf{N}\mathbb{Z}^D]} w_{\boldsymbol{m}}\Big(\frac{1}{|\mathbf{N}|}\sum_{\boldsymbol{k}\in[\mathbb{Z}^D/\mathbb{Z}^D\mathbf{N}]}\mathrm{e}^{j2\pi\boldsymbol{k}\mathbf{N}^{-1}(\boldsymbol{n}-\boldsymbol{m})}\Big).$$

For this to be $w_{\boldsymbol{n}}$ for any data values $\{w_{\boldsymbol{n}}\}$, the parenthesized quantity must be one when $\boldsymbol{m}=\boldsymbol{n}$ and zero otherwise. But $\boldsymbol{m}=\boldsymbol{n}$ and $\boldsymbol{m}\neq\boldsymbol{n}$ are equivalent to $\boldsymbol{m}$ and $\boldsymbol{n}$ being in the same or different cosets of $\mathbf{N}\mathbb{Z}^D$ in $\mathbb{Z}^D$, as each of $\boldsymbol{m}$ and $\boldsymbol{n}$ is from $\big[\mathbb{Z}^D/\mathbf{N}\mathbb{Z}^D\big]$, which has one element from each coset. But $\boldsymbol{m}$ and $\boldsymbol{n}$ are in the same coset if and only if $\boldsymbol{n}-\boldsymbol{m}\in\mathbf{N}\mathbb{Z}^D$, so the essence of the desired inversion result is

$$\frac{1}{|\mathbf{N}|}\sum_{\boldsymbol{k}\in[\mathbb{Z}^D/\mathbb{Z}^D\mathbf{N}]}\mathrm{e}^{j2\pi\boldsymbol{k}\mathbf{N}^{-1}\boldsymbol{n}} = \begin{cases}1 & \text{if } \boldsymbol{n}\in\mathbf{N}\mathbb{Z}^D,\\ 0 & \text{otherwise.}\end{cases} \tag{A3}$$

Of course for specific $\mathbf{N}$, $\big[\mathbb{Z}^D/\mathbf{N}\mathbb{Z}^D\big]$, and $\big[\mathbb{Z}^D/\mathbb{Z}^D\mathbf{N}\big]$, the direct calculation of (A3) is an alternative to the general proof.

PRELIMINARIES

A Homomorphism and its Kernel

A particularly simple group homomorphism will reduce the needed proof to barely more than intepreting the Fundamental Theorem of Homomorphisms [9] (FTOH) in our context.

Since $|\mathbf{N}|$ is a nonzero integer, set $\mathcal{C}_{\mathbf{N}} \triangleq \{\mathrm{e}^{j2\pi u/|\mathbf{N}|} : u\in\mathbb{Z}\}$ is a finite cyclic group under complex multiplication. For brevity let $\mathcal{G}\triangleq\big[\mathbb{Z}^D/\mathbb{Z}^D\mathbf{N}\big]$, a group under modulo-$\mathbf{N}$ addition $\oplus$ defined by $\boldsymbol{k}_1\oplus\boldsymbol{k}_2\triangleq\boldsymbol{k}_1+\boldsymbol{k}_2+\boldsymbol{k}_\Delta\mathbf{N}\in\mathcal{G}$ by unique choice of $\boldsymbol{k}_\Delta\in\mathbb{Z}^D$. Define map $\phi_{\boldsymbol{n}}\colon\mathcal{G}\to\mathcal{C}_{\mathbf{N}}$ by $\phi_{\boldsymbol{n}}(\boldsymbol{k})\triangleq\mathrm{e}^{j2\pi\boldsymbol{k}\mathbf{N}^{-1}\boldsymbol{n}}$. Since $\phi_{\boldsymbol{n}}(\boldsymbol{k}_1\oplus\boldsymbol{k}_2)=\mathrm{e}^{j2\pi(\boldsymbol{k}_1+\boldsymbol{k}_2+\boldsymbol{k}_\Delta\mathbf{N})\mathbf{N}^{-1}\boldsymbol{n}}=\phi_{\boldsymbol{n}}(\boldsymbol{k}_1)\phi_{\boldsymbol{n}}(\boldsymbol{k}_2)$ for every $\boldsymbol{k}_1,\boldsymbol{k}_2\in\mathcal{G}$, map $\phi_{\boldsymbol{n}}$ is a homomorphism [9, Section 1.9]. The group identity in $\mathcal{C}_{\mathbf{N}}$ is unity, so $\phi_{\boldsymbol{n}}$ has kernel $\mathcal{K}\triangleq\{\boldsymbol{k}\in\mathcal{G}\colon\phi_{\boldsymbol{n}}(\boldsymbol{k})=1\}$. (Remember that $\mathcal{K}$ depends on $\boldsymbol{n}$.)

Condition $\boldsymbol{n}\in\mathbf{N}\mathbb{Z}^D$ in (A3) *is Equivalent to $\mathcal{K}=\mathcal{G}$*

Somewhat trivially, if $\boldsymbol{n}\in\mathbf{N}\mathbb{Z}^D$ so that $\boldsymbol{n}=\mathbf{N}\boldsymbol{n}'$ for some $\boldsymbol{n}'\in\mathbb{Z}^D$, then $\boldsymbol{k}\mathbf{N}^{-1}\boldsymbol{n}=\boldsymbol{k}\boldsymbol{n}'\in\mathbb{Z}$ for all $\boldsymbol{k}\in\mathcal{G}$, so $\mathcal{K}=\mathcal{G}$.

Now suppose instead that $\boldsymbol{n}\notin\mathbf{N}\mathbb{Z}^D$ so that $\mathbf{N}^{-1}\boldsymbol{n}$ has a noninteger element. Let $\boldsymbol{k}'\in\mathbb{Z}^D$ be a standard unit vector that gives $\boldsymbol{k}'\mathbf{N}^{-1}\boldsymbol{n}$ that noninteger value. Coset decomposition $\boldsymbol{k}'=\boldsymbol{k}+\boldsymbol{k}''\mathbf{N}$ with unique $\boldsymbol{k}\in\mathcal{G}$ and $\boldsymbol{k}''\in\mathbb{Z}^D$ yields $\boldsymbol{k}\mathbf{N}^{-1}\boldsymbol{n}=\boldsymbol{k}'\mathbf{N}^{-1}\boldsymbol{n}-\boldsymbol{k}''\boldsymbol{n}\notin\mathbb{Z}$, a counterexample that disproves $\mathcal{K}=\mathcal{G}$.

From $|\mathcal{G}|=|\mathbf{N}|$ and the above then, (A3) is equivalent to

$$\sum_{\boldsymbol{k}\in\mathcal{G}}\mathrm{e}^{j2\pi\boldsymbol{k}\mathbf{N}^{-1}\boldsymbol{n}} = \begin{cases}|\mathcal{K}| & \text{if } \mathcal{K}=\mathcal{G},\\ 0 & \text{otherwise.}\end{cases} \tag{A4}$$

THE ACTUAL PROOF

With the preliminaries now in place, let us prove (A4) and therefore that the IDFT inverts the DFT. Kernel $\mathcal{K}$ is (FTOH) a normal subgroup of $\mathcal{G}$, so we can choose family $[\mathcal{G}/\mathcal{K}] \subset \mathcal{G}$ of representatives of cosets of $\mathcal{K}$ in $\mathcal{G}$. Coset decomposition of its index then makes the sum in (A4) just

$$\begin{aligned}\sum_{\boldsymbol{k}\in\mathcal{G}} \mathrm{e}^{j2\pi \boldsymbol{k}\mathbf{N}^{-1}\boldsymbol{n}} &= \sum_{\boldsymbol{\ell}\in[\mathcal{G}/\mathcal{K}]} \sum_{\boldsymbol{k}\in\mathcal{K}} \phi_{\boldsymbol{n}}(\boldsymbol{\ell}\oplus\boldsymbol{k}) = \sum_{\boldsymbol{k}\in\mathcal{K}} \sum_{\boldsymbol{\ell}\in[\mathcal{G}/\mathcal{K}]} \phi_{\boldsymbol{n}}(\boldsymbol{\ell})\phi_{\boldsymbol{n}}(\boldsymbol{k}) \\ &= |\mathcal{K}| \sum_{\boldsymbol{\ell}\in[\mathcal{G}/\mathcal{K}]} \phi_{\boldsymbol{n}}(\boldsymbol{\ell}) \end{aligned} \tag{A5}$$

as $\phi_{\boldsymbol{n}}(\boldsymbol{k}) = 1$. If we partition $\mathcal{G}$ into the actual family of cosets

$$\mathcal{G}/\mathcal{K} = \left\{\boldsymbol{\ell}\oplus\mathcal{K}\colon \boldsymbol{\ell} \in \left[\mathcal{G}/\mathcal{K}\right]\right\}$$

represented by $\left[\mathcal{G}/\mathcal{K}\right]$ (note $\mathcal{G}/\mathcal{K}$ is independent of the representatives chosen for $\left[\mathcal{G}/\mathcal{K}\right]$, a standard, easy-to-prove fact), image $\phi_{\boldsymbol{n}}(\mathcal{G})$ is (FTOH) isomorphic to $\mathcal{G}/\mathcal{K}$ and so has the same number $N \triangleq |\mathcal{G}|/|\mathcal{K}|$ of elements. The image comprises the values taken by $\phi_{\boldsymbol{n}}(\boldsymbol{\ell}\oplus\boldsymbol{k})$ for all combinations of $\boldsymbol{\ell} \in [\mathcal{G}/\mathcal{K}]$ and $\boldsymbol{k} \in \mathcal{K}$, but since $\phi_{\boldsymbol{n}}(\boldsymbol{\ell}\oplus\boldsymbol{k}) = \phi_{\boldsymbol{n}}(\boldsymbol{\ell})\phi_{\boldsymbol{n}}(\boldsymbol{k}) = \phi_{\boldsymbol{n}}(\boldsymbol{\ell})$, the image must also comprise exactly the N terms of the sum in (A5). The image, of $\phi_{\boldsymbol{n}}\colon \mathcal{G} \to \mathcal{C}_{\mathbf{N}}$, is (FTOH) a subgroup of cyclic group $\mathcal{C}_{\mathbf{N}}$, making it cyclic [9, Thm 1.3] as well. In (A5) then, the terms are $1, a, ..., a^{N-1}$ for some generator a.

If $\mathcal{K} = \mathcal{G}$, the sum in (A5) has $N = 1$ term, so $\boldsymbol{\ell} \in \mathcal{K}$ and $\phi_{\boldsymbol{n}}(\boldsymbol{\ell}) = 1$. The sum is one, so the $\mathcal{K} = \mathcal{G}$ arm of (A4) is proved.

If $\mathcal{K} \neq \mathcal{G}$, kernel $\mathcal{K}$ is a proper subgroup of $\mathcal{G}$, so $N > 1$, generator $a \neq 1$, and the sum in (A5) is a finite geometric series with value $(1 - a^N)/(1 - a)$. But $a^N = 1$ for any group element a in an N-element cyclic multiplicative group [9, Thm. 1.4], so the series equals zero. This proves the $\mathcal{K} \neq \mathcal{G}$ arm of (A4).